Journal of Power Sources 201 (2012) 253–258

Contents lists available at SciVerse ScienceDirect

Journal of Power Sources

journal homepage: www.elsevier.com/locate/jpowsour

Preparation and electrochemical performance of Gd-doped $LiFePO_4$/C composites

Lijuan Pang[a], Minshou Zhao[a,c,*], Xian Zhao[b], Yujun Chai[d]

[a] College of Environmental and Chemical Engineering, Yanshan University, Qinhuangdao 066004, China
[b] College of Chemistry and Chemical Engineering, Shanghai Jiaotong University, Shanghai 200240, China
[c] State Key Laboratory of Metastable Material Science and Technology, Yanshan University, Qinhuangdao 066004, China
[d] Department of Chemistry and Materials Science, Heibei Normal University, Shijiazhuang 050016, China

ARTICLE INFO

Article history:
Received 4 July 2011
Received in revised form 20 October 2011
Accepted 25 October 2011
Available online 3 November 2011

Keywords:
Lithium-ion battery
Lithium iron phosphate
Gadolinium ion-doped
Electrochemical performance
Low temperature

ABSTRACT

In this paper, $LiFe_{1-x}Gd_xPO_4$/C composites (x = 0, 0.02, 0.04, 0.06, 0.07, 0.08) are synthesized *via* a high-temperature solid-phase reaction. The structure and electrochemical behavior of the materials are investigated using a wide range of techniques such as X-ray diffraction (XRD), scanning electron microscope (SEM), energy dispersive spectroscopy (EDS), particle size analysis, galvanostatic charge/discharge and electrochemical impedance spectroscopy (EIS). It is found that the maximum discharge capacity of the as-prepared $LiFe_{0.93}Gd_{0.07}PO_4$/C composite can reach up to 150.7 mAh g^{-1}, 125.9 mAh g^{-1}, 106.0 mAh g^{-1} and 81.3 mAh g^{-1} at rates of 0.2 C, 1 C, 5 C and 10 C, respectively. And at 0.1 C rate, the initial discharge capacity of the composite monotonically increases with temperature from 66.3 to 122.2 mAh g^{-1} in the range of −30 to 0 °C. It is also demonstrated that the presence of a small amount of Gd^{3+} ion in the sample prepared in this work can reduce the charge-transfer resistance, resulting in the enhanced electrochemical catalytic activity.

1. Introduction

Since the pioneering work of Padhi and co-workers in 1997 [1], $LiFePO_4$, one of the most attractive cathode material, has received an extensive interests over the past decade due to cell safety, low cost, low toxicity, stable voltage platform and long cycle life. For pure $LiFePO_4$, the intrinsic disadvantages of poor electronic conductivity and slow diffusion coefficient of lithium ion [1,2] has been demonstrated to be the predominant restriction to the high-rate performance of cell, which is open to address all around the world.

Up to the present, two techniques have been proposed to improve the electrochemical performance of $LiFePO_4$. One is coating carbon on its surface [3]. Huang et al. [4] reported that $LiFePO_4$/C composite demonstrated excellent electrochemical property. The discharge capacity was 150 and 120 mAh g^{-1} at a rate of 0.2 C and 5 C, respectively. Chen and Dahn [5] reported that the capacity of $LiFePO_4$/C reached 160 mAh g^{-1} at 0.1 C rate, which was closed to the theoretical capacity.

The second method is to dope metal ion, which has been considered as an efficient way for the enhancement of the electrochemical performance of $LiFePO_4$. Many elements have been used to dope $LiFePO_4$ as $Li_{1-x}M_xFePO_4$ [6–10] or $LiFe_{1-x}M_xPO_4$ [11] (x = 0–1). However, the electrochemical performance of $LiFePO_4$ needs improvement to meet the requirement for practical lithium ion batteries as power or energy storage sources in the future. It has been reported that Cho et al. [12] synthesized $LiFe_{1-x}La_xPO_4$/C by a solid-state reaction. It was indicated that these La-ion dopants had no effect on the structure of the material. Instead, it considerably improved its rate capacity performance and cyclic stability. Among the materials, $LiFe_{0.99}La_{0.01}PO_4$/C presented the best electrochemical behavior, with a discharge capacity of 156 mAh g^{-1} at a rate of 0.2 C. Zhao et al. [13] synthesized $LiFe_{1-x}Nd_xPO_4$/C (x = 0–0.08), and $LiFe_{0.96}Nd_{0.06}PO_4$/C delivered the highest discharge capacity of 165.2 mAh g^{-1}, 146.8 mAh g^{-1}, 125.7 mAh g^{-1} and 114.8 mAh g^{-1} at rates of 0.2 C, 1 C, 2 C and 5 C, respectively. According to Saiful Islam et al. [14], the energy of dopant substitution or the "solution" reaction can be calculated by combining the appropriate defect and lattice energy. The calculated results showed that for all trivalent dopants on Fe, the lowest energy was found for Nd^{3+} ion.

Demonstrated mentioned above, doping appropriate metal ions into $LiFePO_4$ is a very effective method to improve the performances of $LiFePO_4$.

Gd element has a special electronic structure (4f electron shell of half full), and we expected that doping Gd^{3+} ion will be beneficial for enhancing performances of $LiFePO_4$. In this paper, we have synthesized $LiFe_{1-x}Gd_xPO_4$/C sample by a high temperature solid-phase reaction and its electrochemical performance has been characterized first time.

* Corresponding author at: College of Environmental and Chemical Engineering, Yanshan University, Qinhuangdao 066004, China. Tel.: +86 335 8074730; fax: +86 335 8061569.
E-mail addresses: zhaoms@ysu.edu.cn, zlplj1113@126.com (M. Zhao).

0378-7753/$ – see front matter © 2011 Elsevier B.V. All rights reserved.
doi:10.1016/j.jpowsour.2011.10.096

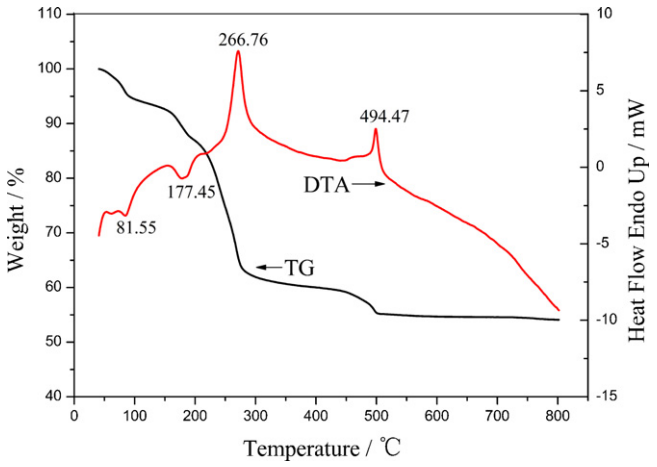

Fig. 1. TG-DTA curves of $LiFe_{0.93}Gd_{0.07}PO_4/C$ precursor.

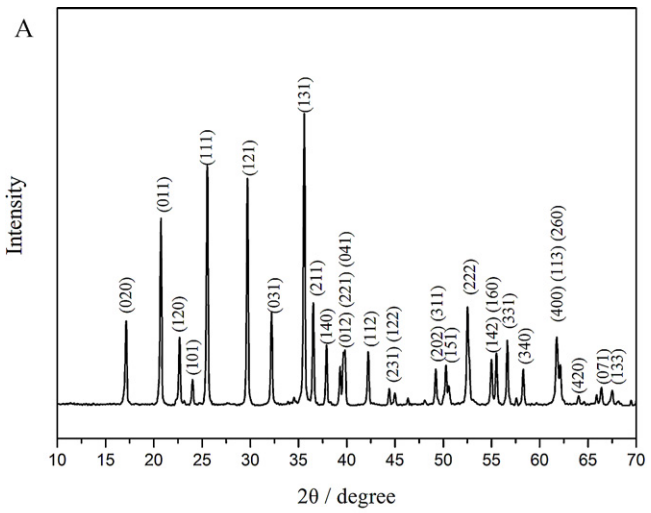

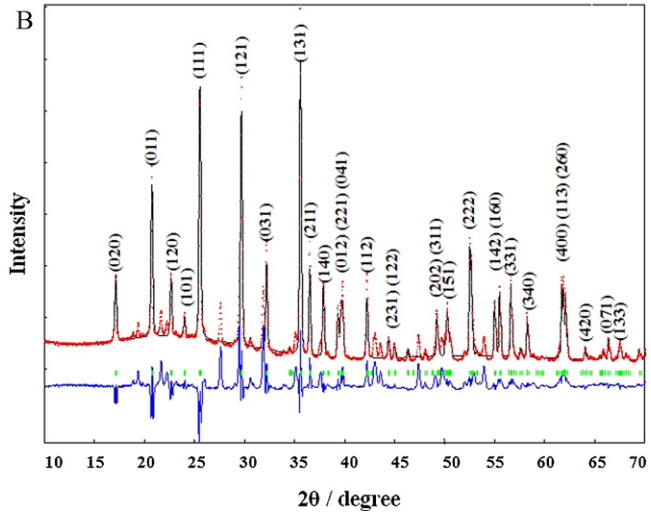

Fig. 2. (A) XRD pattern for $LiFePO_4/C$ composite. (B) Rietveld refinement of XRD pattern for $LiFe_{0.93}Gd_{0.07}PO_4/C$ composite.

2. Experimental

$LiFe_{1-x}Gd_xPO_4/C$ composites ($x = 0$, 0.02, 0.04, 0.06, 0.07, 0.08) were synthesized using $CH_3COOLi{\cdot}2H_2O$ (AR), $FeC_2O_4{\cdot}2H_2O$ (AR), $NH_4H_2PO_4$ (AR) and Gd_2O_3 (99.9%) as the raw materials in the mole ratio based on the formula of $LiFePO_4$. The starting materials, with added 5 wt.% glucose and a proper amount of anhydrous ethanol, were milled by ball-milling (ball to powder weight ratio of 15:1) for 12 h and dried using a hair driver. Then, the precursors were heat-treated at 350 °C for 6 h and 700 °C for 16 h under N_2 atmosphere, respectively.

The thermal behavior of precursor was analyzed using Themogravimetric apparatus (Pyris Diamond, PerkinElmer Thermal Analysis) under nitrogen flow. The sample was heated from ambient temperature to 800 °C at the rate of 10 °C min^{-1}. To identify the structure of the sample, the structure of the powder was performed with XRD on a Rigaku D/max-2500/pc. Laser particle size analyzer was applied to analyze the particle size of the sample. The morphology of sample was observed using a field-emission scanning electron microscope (FE-SEM) on S-4800 FE-SEM. The S-4800 FE-SEM is equipped with EDS, which is used to analyze the elemental composition.

The electrochemical performance of the sample was measured in a simulative cell with a lithium metal as anode electrode. The working electrode was produced by dispersing 80 wt.% active material, 15 wt.% acetylene black and 5 wt.% polyvinylidene fluoride (PVDF) binder in N-methylpyrrolidione (NMP) solvent to form a uniform slurry. The slurry was coated on Al foil and dried in a vacuum at 120 °C for 12 h. Celgard 2400 was used as a separator. The electrolyte was 1M $LiPF_6$/EC + DEC (1:1, v/v). The cell was tested over the voltage range 2.5–4.2 V.

3. Result and discussion

Fig. 1 shows the TG-DTA curves of $LiFe_{0.93}Gd_{0.07}PO_4/C$ composite. The weight loss at 81 °C corresponds to the loss of remaining ethanol and adsorbed water in the precursor. The weight loss in the temperature region of 81–155 °C is related to the dehydration $CH_3COOLi{\cdot}2H_2O$ and $FeC_2O_4{\cdot}2H_2O$. The main weight loss in the temperature ranges of 190–280 °C and 280–430 °C are described to the decomposition of $NH_4H_2PO_4$ and FeC_2O_4, respectively. The DTA curve shows a small endothermic peak at 177.45 °C and two exothermic peaks, which is located at 266.76 °C and 494.47 °C respectively. The obvious peak, located at 266.76 °C, is related to the formation of $LiFePO_4$ compound, and the other smaller peak is located at 494.47 °C, where a new solid-state reaction occurs with the transformation of crystalline material [15]. While further enhancing up temperature, the TG curve almost keeps a constant value until 800 °C. Therefore, the temperature for synthesizing $LiFe_{0.93}Gd_{0.07}PO_4/C$ should be higher than 500 °C.

Fig. 2A and B shows the XRD pattern of $LiFePO_4/C$ composite and Rietveld refinement of the XRD pattern for $LiFe_{0.93}Gd_{0.07}PO_4/C$ composite, respectively. The observed pattern and calculated pattern match well in Fig. 2B. The crystal phases of two samples are olivine structure indexed by orthorhombic Pnma. These results suggest that a small amount of Gd^{3+} ion-doped does not affect the olivine structure of $LiFePO_4$. In addition, a carbon diffraction peak does not be observed in Fig. 2A and B, which implies that the micro-carbon coating does not also affect the structure of $LiFePO_4$. However, XRD pattern of Gd-doped $LiFePO_4$ shows more Bragg reflections than Gd-free $LiFePO_4$ because the ionic radius of Gd^{3+} ion doped (0.0938 nm) is larger than that of Fe^{2+} ion (0.078 nm), leading to bigger unit cell parameters, as shown in Table 1. Table 1 lists the unit cell parameters obtained from Rietveld refinement of the XRD for $LiFe_{0.93}Gd_{0.07}PO_4/C$ and unit cell parameters of $LiFePO_4/C$. Results of Rietveld refinement confirm that Gd^{3+} ion has been successfully doped into $LiFePO_4/C$. Clearly, doping a small amount of Gd^{3+} ion has little effect on the cell parameters of $LiFePO_4$. However, the dopant of a larger ionic radius perhaps

Table 1
Unit cell parameters obtained from Rietveld refinement of XRD for $LiFe_{0.93}Gd_{0.07}PO_4$/C and unit cell parameters of $LiFePO_4$/C.

Sample	a (nm)	b (nm)	c (nm)
$LiFePO_4$/C	1.0324	0.6007	0.4695
$LiFe_{0.93}Gd_{0.07}PO_4$/C	1.0471	0.6092	0.4758

Table 2
Element composition in $LiFe_{0.93}Gd_{0.07}PO_4$/C.

Element	C (K)	O (K)	P (K)	Fe (K)	Gd (L)	Total
W%	5.40	42.23	16.83	29.77	5.77	100.00
A%	10.71	62.81	12.93	12.68	0.87	100.00

creates the more defects in $LiFePO_4$, which is beneficial for the electrochemical catalytic activity of the electrode.

The grain size of samples can be described by particle size distribution. Fig. 3 presents the particle size distributions of $LiFePO_4$/C sample and $LiFe_{0.93}Gd_{0.07}PO_4$/C sample, respectively. Fig. 4 depicts the FE-SEM images of $LiFePO_4$/C sample and $LiFe_{0.93}Gd_{0.07}PO_4$/C sample, respectively. It is apparent from Figs. 3 and 4 that the particle size of $LiFe_{0.93}Gd_{0.07}PO_4$/C sample is significantly smaller than that of $LiFePO_4$/C sample, and the particle scale is uniform after doping Gd^{3+} ion, which indicates that doping a small amount of Gd^{3+} can effectively reduce the particle size of $LiFePO_4$/C and make it more uniform.

The EDS image of $LiFe_{0.93}Gd_{0.07}PO_4$/C is shown in Fig. 5. The compositions of the substituent elements are listed in Table 2. The result shows the atomic ratio of Fe, Gd, P and O is 0.981:0.067:1:4.858 in $LiFe_{0.93}Gd_{0.07}PO_4$/C sample, essentially coinciding with $LiFe_{0.93}Gd_{0.07}PO_4$/C. Wagemaker et al. [16] studied the supervalent-cation dopant in $LiFePO_4$ by combining neutron and X-ray diffraction. The results showed that low levels of dopants were indeed soluble in the olivine lattice up to the extent of 3 mol%. Therefore, we infer that Gd^{3+} ion occupies Fe^{2+} ion site in $LiFePO_4$/C or has been dissolved into $LiFePO_4$/C to form a solid solution.

The cycle performance of $LiFe_{1-x}Gd_xPO_4$/C samples (x = 0, 0.02, 0.04, 0.06, 0.07, 0.08) at a rate of 0.2 C is shown in Fig. 6A. With increasing amount of Gd^{3+} ion doped, the discharge capacity becomes higher, but the discharge capacity decreases when the doping amount is 8%. We conclude that the sample has the best electrochemical performance when the amount of Gd^{3+} ion doped is 7%. Fig. 6B shows the charge–discharge curves of $LiFePO_4$/C sample and $LiFe_{0.93}Gd_{0.07}PO_4$/C sample at 0.2 C rate, respectively, which shows a wider voltage platform and a smaller gap between the charge and discharge curves after doping Gd^{3+} ion. This result

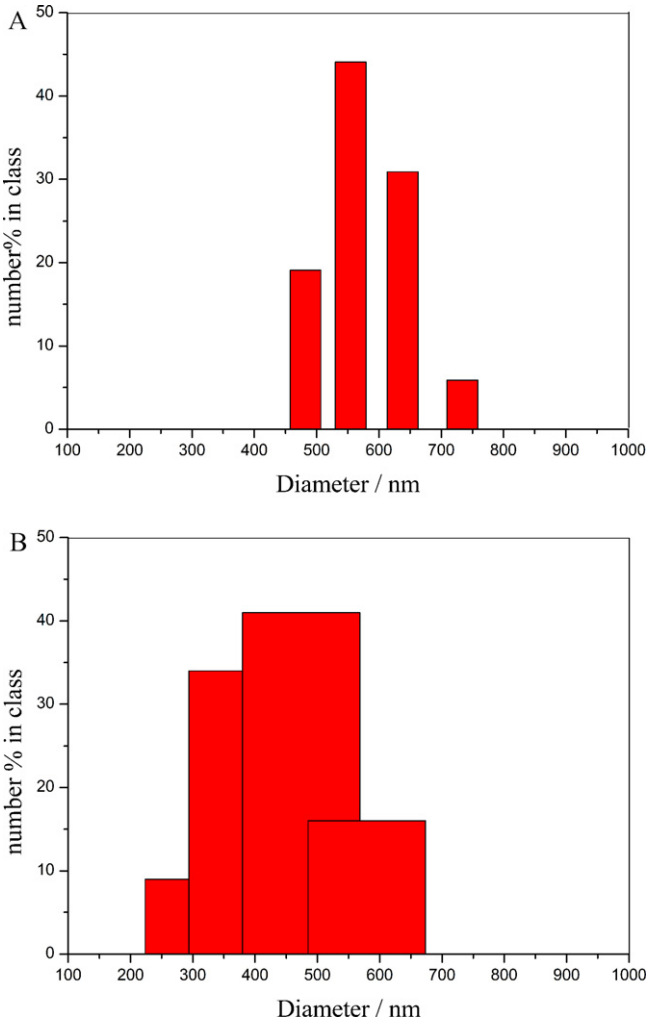

Fig. 3. A Particle size distribution of $LiFePO_4$/C. (B) Particle size distribution of $LiFe_{0.93}Gd_{0.07}PO_4$/C.

indicates that the charge–discharge efficiency and reversibility are significantly improved.

The cycle performance of $LiFe_{0.93}Gd_{0.07}PO_4$/C sample at various rates is shown in Fig. 7A. The maximum discharge capacity is 150.7 mAh g^{-1}, 125.9 mAh g^{-1}, 106.0 mAh g^{-1} and 81.3 mAh g^{-1} at rates of 0.2 C, 1 C, 5 C and 10 C, respectively.

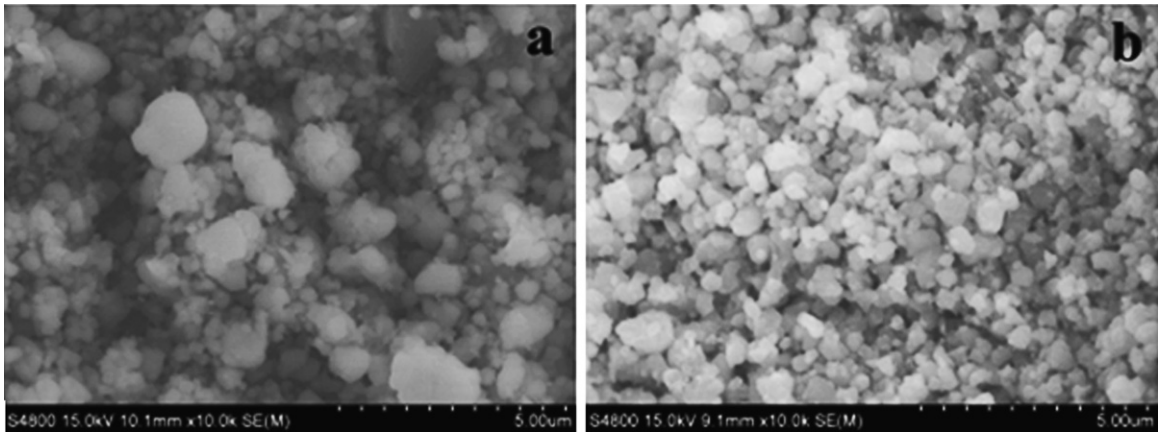

Fig. 4. FE-SEM images of $LiFePO_4$/C (a) and $LiFe_{0.93}Gd_{0.07}PO_4$/C (b).

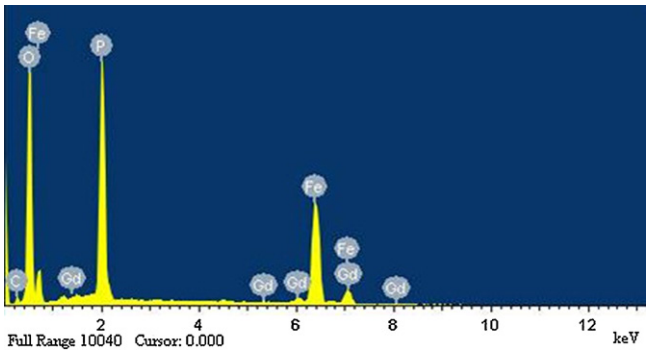

Fig. 5. EDS image of $LiFe_{0.93}Gd_{0.07}PO_4/C$.

Fig. 7B shows the discharge curves of $LiFe_{0.93}Gd_{0.07}PO_4/C$ sample at various rates. It is concluded that doping an appropriate amount of Gd^{3+} ion can improve the high-rate discharge performance of $LiFePO_4/C$ composite.

It is inferred that doping Gd^{3+} ion can reduce the particle size of $LiFePO_4/C$, shorten the transport path of Li^+ ion, increase the disorder of the lattice and create the defect in $LiFePO_4/C$. These factors would improve the electrochemical performance of $LiFePO_4/C$ composite.

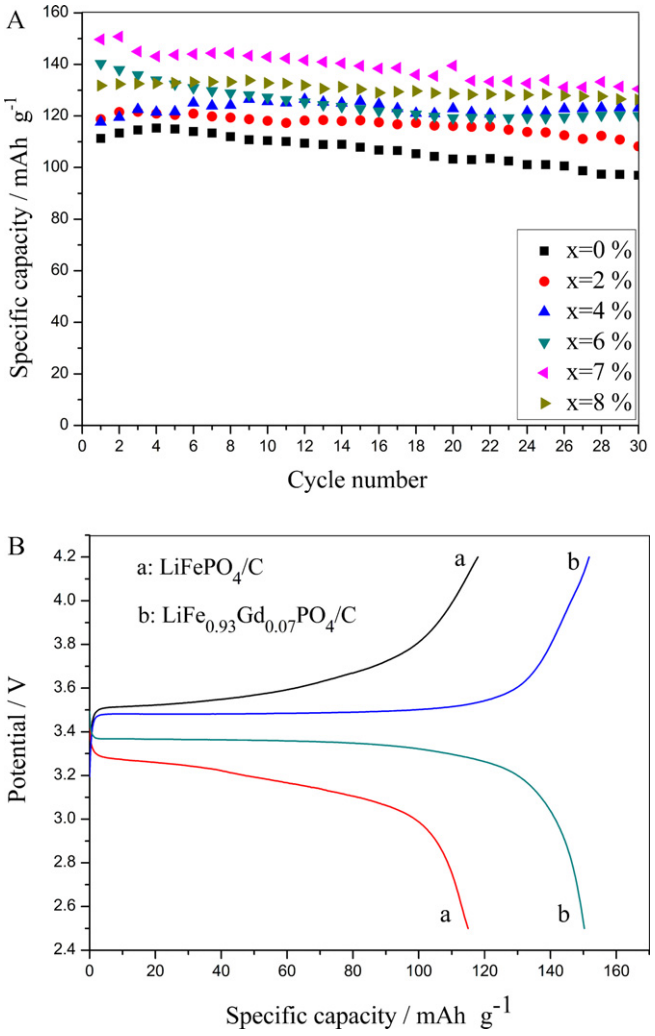

Fig. 6. (A) Discharge capacity as a function of cycle number for $LiFePO_4/C$ and $LiFe_{1-x}Gd_xPO_4/C$ (x = 0–0.08) at a rate of 0.2 C. (B) Second charge–discharge curves of $LiFePO_4/C$ and $LiFe_{0.93}Gd_{0.07}PO_4/C$ at a rate of 0.2 C.

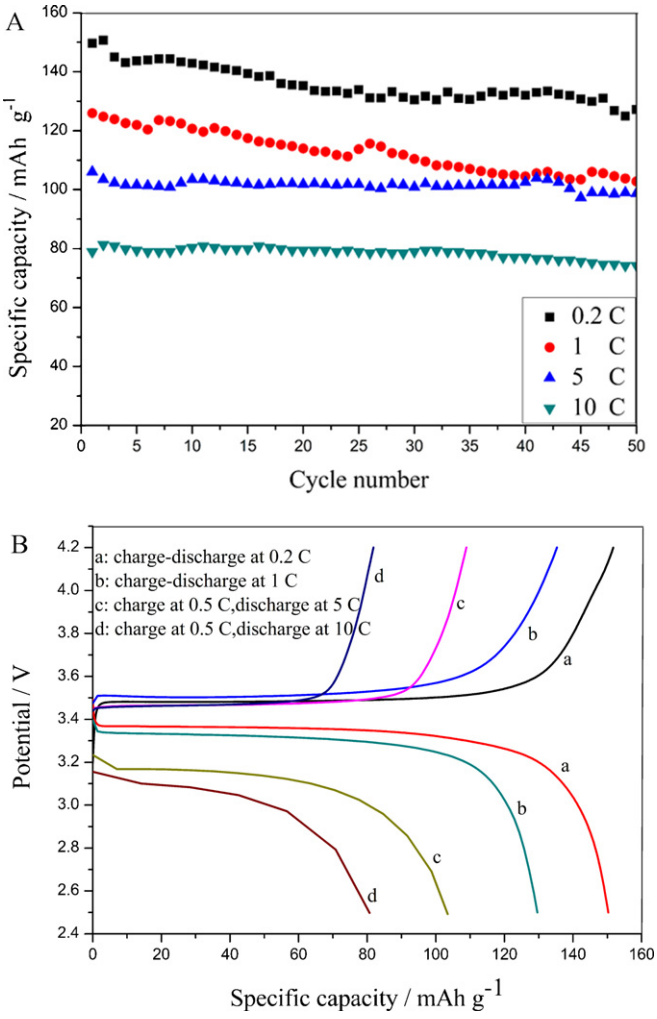

Fig. 7. A Discharge capacity as a function of cycle number for $LiFe_{0.93}Gd_{0.07}PO_4/C$ at various rates. (B) Second charge–discharge curves of $LiFe_{0.93}Gd_{0.07}PO_4/C$ at various rates.

The electrochemical measurements have also been carried out at lower temperatures, as shown in Fig. 8. And at 0.1 C rate, the initial discharge capacity is 122.2 mAh g^{-1}, 107.7 mAh g^{-1}, 80.4 mAh g^{-1} and 66.3 mAh g^{-1} at 0 °C, −10 °C, −20 °C and −30 °C respectively. The discharge capacity monotonously sharply decreases with decreasing temperature, just as expected. At lower temperature the transport speed of Li^+ ion slows down and polarization influence becomes more dominant. These perhaps are key issues.

EIS was used to further analyze the effect of doping Gd^{3+} ion on the electrode reaction impedance. Before EIS tests, the electrodes were cycled galvanostatically for three cycles. Fig. 9 shows EIS of $LiFePO_4/C$ electrode reaction and $LiFe_{0.93}Gd_{0.07}PO_4/C$ electrode reaction at 15 °C. An equivalent circuit model (Fig. 10) was constructed to analyze the impedance spectra. In Fig. 9, EIS is composed of two partially overlapped circles at high frequency region and a straight line at low frequency region. An intercept at Z_{real} axis at high frequency represents the ohmic resistance (Rs), which consists of the resistances of the electrolyte and electrode. The semicircle at high frequency region represents the migration of Li^+ ion at the electrode/electrolyte interface *via* the SEI layer and the semicircle at middle frequency range indicates the charge-transfer resistance, which corresponds to Rct in the equivalent circuit, as shown in Fig. 10. The straight line in low frequency region is ascribed to the diffusion of Li^+ ion in the electrode material and called Warburg

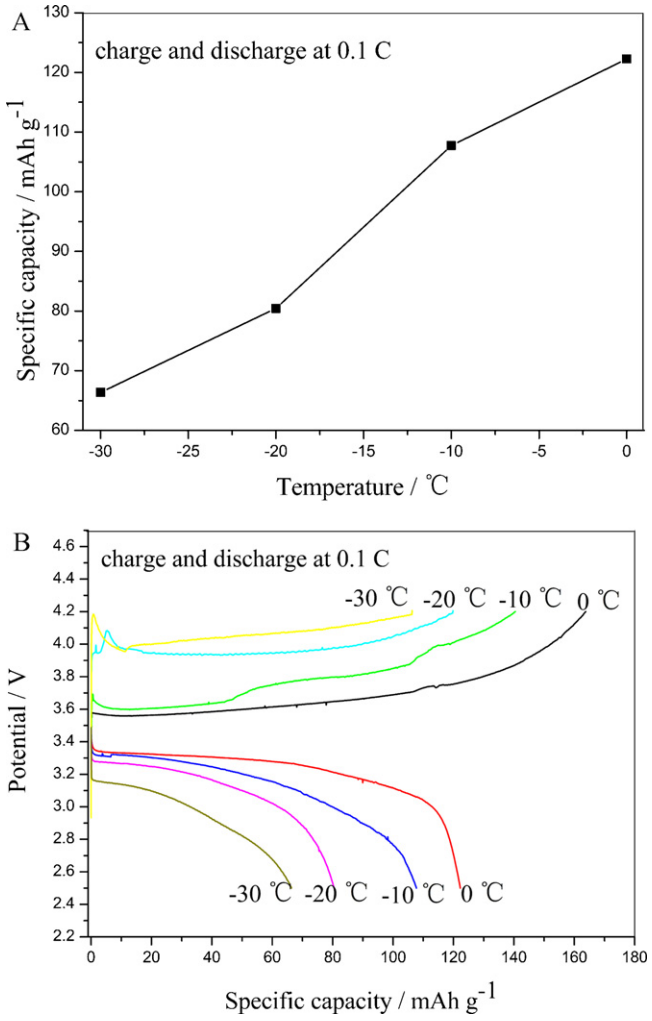

Fig. 8. A Initial discharge capacity for $LiFe_{0.93}Gd_{0.07}PO_4/C$ at various temperatures. (B) Initial charge–discharge curves of $LiFe_{0.93}Gd_{0.07}PO_4/C$ at various temperatures.

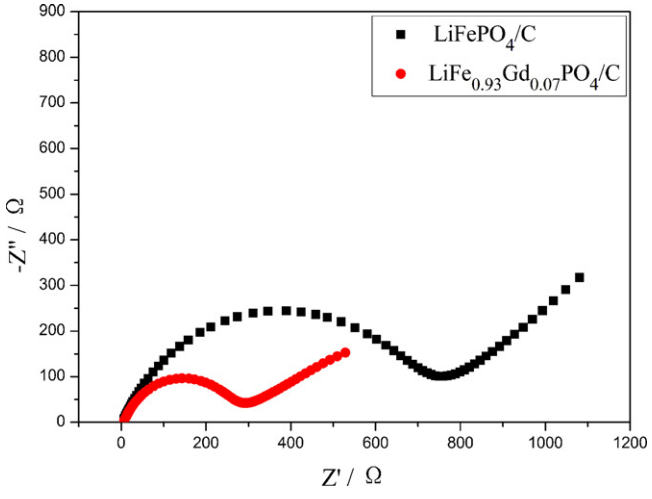

Fig. 9. EIS for $LiFePO_4/C$ electrode and $LiFe_{0.93}Gd_{0.07}PO_4/C$ electrode after 3 cycles.

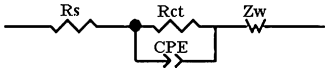

Fig. 10. Equivalent circuit for fitting experimental EIS data.

Table 3
Electrochemical impedance and exchange current density.

Sample	Rs (Ω)	Rct (Ω)	I_0 (mA g^{-1})
$LiFePO_4/C$	3.406	692.6	26.3
$LiFe_{0.93}Gd_{0.07}PO_4/C$	3.288	241.3	128.5

impedance, which corresponds to Zw in Fig. 10. In Fig. 10, a constant phase element (CPE) represents the double layer capacitance and passivation film capacitance [17].

The results were obtained using Zview software and are listed in Table 3. The ohmic resistance (Rs) does not almost change for two samples, because the same electrolyte was used when the simulative cells were assembled. As expected, charge-transfer impedance obviously decreases in the charge–discharge process because of the addition of Gd^{3+} ion. The charge transfer resistance (Rct) for $LiFePO_4/C$ electrode reaction and $LiFe_{0.93}Gd_{0.07}PO_4/C$ electrode reaction is 692.6 Ω and 241.3 Ω, respectively. This great decrease in the impedance will benefit to overcome the restriction of kinetics in the charge–discharge process and improve the cycling performance of the material [18].

An apparent exchange current density (I_0) can be often used to sign the catalytic activity of electrode, which is an important parameter of kinetics for an electrochemical reaction. It can be calculated using Formula (1) [19] when overpotential is very small, and the results are also listed in Table 3.

$$I_0 = \frac{R \cdot T}{n\mathrm{Rct} \cdot F} \quad (1)$$

where R is gas constant, T is absolute temperature, F is Faraday constant, n is charge-transfer number and Rct is charge-transfer resistance.

I_0 for $LiFePO_4/C$ electrode and $LiFe_{0.93}Gd_{0.07}PO_4/C$ electrode is 26.3 mA g^{-1} and 128.5 mA g^{-1}, respectively. This result implies that the catalytic activity of the $LiFe_{0.93}Gd_{0.07}PO_4/C$ electrode is higher than that of $LiFePO_4/C$ electrode, which is why $LiFe_{0.93}Gd_{0.07}PO_4/C$ composite has better electrochemical performance. EIS results indicate that doping an appropriate amount of Gd^{3+} ion can improve the electrochemical activity of $LiFePO_4/C$ composite.

4. Conclusions

Olivine structured $LiFe_{1-x}Gd_xPO_4/C$ composites (x = 0, 0.02, 0.04, 0.06, 0.07, 0.08) have been synthesized by a high temperature solid-state reaction. The electrochemical test results show that $LiFe_{0.93}Gd_{0.07}PO_4/C$ sample demonstrates excellent electrochemical performance with the maximum discharge capacity of 150.7 mAh g^{-1}, 125.9 mAh g^{-1}, 106.0 mAh g^{-1} and 81.3 mAh g^{-1} at rates of 0.2 C, 1 C, 5 C and 10 C, respectively. And at 0.1 C rate, the initial discharge capacity is 122.2 mAh g^{-1}, 107.7 mAh g^{-1}, 80.4 mAh g^{-1} and 66.3 mAh g^{-1} at 0 °C, −10 °C, −20 °C and −30 °C respectively. EIS results indicate that the charge-transfer resistance of electrode reaction greatly decreases by doping an appropriate amount of Gd^{3+} ion. It is inferred that Gd^{3+} ion occupies Fe^{2+} ion site in $LiFePO_4/C$ or has been dissolved into $LiFePO_4/C$ to form a solid solution.

Acknowledgement

This work was financially supported by the Natural Science Foundation of Hebei Province (grant number: B2011203074).

References

[1] A.K. Padhi, K.S. Nanjundaswamy, J.B. Goodenough, J. Electrochem. Soc. 144 (1997) 1188–1194.
[2] S.J. Kwon, C.W. Kim, T.J. Woon, K.S. Lee, J. Power Sources 137 (2004) 93–99.

[3] N. Ravet, Y. Chouinard, J.F. Magnan, S. Besner, M. Gauthier, M. Armand, J. Power Sources 97–98 (2001) 503–507.
[4] H. Huang, S.C. Yin, L.F. Nazar, Solid State Lett. 4 (2001) A170–A172.
[5] Z.H. Chen, J.R. Dahn, J. Electrochem. Soc. 149 (2002) A1184–A1189.
[6] K.F. Hsu, S.Y. Tsay, B.J. Hwang, J. Power Sources 146 (2005) 529–533.
[7] J. Yao, K. Konstantinov, G.X. Wang, H.K. Liu, J. Solid State Electrochem. 11 (2007) 177–185.
[8] G.X. Wang, S.L. Bewlay, K. Konstantinov, H.K. Liu, S.X. Dou, J.H. Ahn, Electrochim. Acta 50 (2004) 443–447.
[9] X. Yin, K. Huang, S. Liu, H. Wang, H. Wang, J. Power Sources 195 (2010) 4308–4312.
[10] G. Wang, Y. Cheng, M. Yan, Z. Jiang, J Solid State Electrochem. 11 (2007) 457–462.
[11] D. Wang, Li S H., S. Shi, X. Huang, Chen S L., Electrochim. Acta 50 (2005) 2955–2958.
[12] Y.-D. Cho, G.T.-K. Fey, H.-M. Kao, J. Solid State Electrochem. 12 (2008) 815–823.
[13] X. Zhao, X. Tang, L. Zhang, M. Zhao, J. Zhai, Electrochim. Acta 55 (20) (2010) 5899–5904.
[14] M. Saiful Islam, D.J. Driscoll, C.A.J. Fisher, P.R. Slater, Chem. Mater. 17 (2005) 5085–5092.
[15] B.L. Yu, J.D. Jiang, Applied Thermal Analysis, Textile Industry Press, Beijing, 1990, p. 114.
[16] M. Wagemaker, L.E. Brian, D. Lützenkirchen-Hecht, F.M. Mulder, L.F. Nazar, Chem. Mater. 20 (2008) 6313–6315.
[17] G.X. Wang, L. Yanga, Y. Chena, J.Z. Wanga, S. Bewlaya, H.K. Liua, Electrochim. Acta 50 (2005) 4649–4654.
[18] S.T. Yang, Y.X. Liu, Y.H. Yin, H. Wang, T. Wang, Chin. J. Inorg. Chem. 23 (2007) 1165–1168.
[19] A.J. Bard, L.R. Faulker, Electrochemical methods-fundamental and applications, L.Y. Gu, M.X. Lu, S.Z. Song, Chinese Version, Chemical Industry Publishing Company, 1986, p. 121.